REPORT DOCUMENTATION PAGE

Form Approved
OMB No. 0704-0188

1. AGENCY USE ONLY (Leave blank)	2. REPORT DATE	3. REPORT TYPE AND DATES COVERED
	Sept. 9, 1996	Technical Report #16

4. TITLE AND SUBTITLE
Electrochemical Properties and Electronic Structures of Conjugated Polyquinolines and Polyanthrazolines

5. FUNDING NUMBERS
N00014-94-1-0540

6. AUTHOR(S)
A.K. Agrawal and S.A. Jenekhe

Kenneth J. Wynne
R & T Code: 3132111

7. PERFORMING ORGANIZATION NAME(S) AND ADDRESS(ES)
Department of Chemical Engineering
University of Rochester
206 Gavett Hall
Rochester, NY 14627

8. PERFORMING ORGANIZATION REPORT NUMBER
16

9. SPONSORING/MONITORING AGENCY NAME(S) AND ADDRESS(ES)
Office of Naval Research
800 North Quincy Street
Arlington, VA 22217-5000

10. SPONSORING/MONITORING AGENCY REPORT NUMBER

11. SUPPLEMENTARY NOTES
Published in *Chemistry of Materials*, **8**, 579 - 589 (1996).

12a. DISTRIBUTION/AVAILABILITY STATEMENT
Reproduction in whole or in part is permitted for any purpose of the United States Government.
This document has been approved for public release and sale; its distribution is unlimited.

12b. DISTRIBUTION CODE

13. ABSTRACT *(Maximum 200 words)*

The effects of molecular structure on the electronic structure and redox properties of a series of 22 systematically designed polyquinolines and polyanthrazolines are explored by cyclic voltametry and spectroelectrochemistry on thin films. The measured electrochemical bandgap of the series of conjugated polymers was in the range 2.0-3.1 eV and found to be in good agreement with the optical bandgap. The oxidation and reduction potentials, ionization potential, and electron affinity of the series of polymers were correlated by their main structural features. All the polyquinolines and polyanthrazolines had reversible reduction with formal potentials of -1.57 to -2.08 V (versus SCE) which make them excellent n-type semiconducting polymers. Polymers containing anthrazoline units have a higher electron affinity by 0.3 - 0.4 eV than those containing bis(quinoline) units. On the other hand, thiophene-linked polymers have a lower ionization potential by 0.45 - 0.5 eV than those with phenylene linkages. Thus, thiophene-linked polyanthrazolines combine both low ionization potentials (~4.8 - 4.9 eV) and high electron affinities (~2.9 eV) and as a result can be p-type and n-type doped to conducting polymers with relatively more stability in air. Spectroelectrochemistry of the thiophene-linked revealed features characteristic of polarons and bipolarons or radical ion dimers. The results suggest that the series of polyquinolines and polyanthrazolines are promising electronic and optoelectronic materials.

14. SUBJECT TERMS
Polyquinolines; Polyanthrazolines; electrochemical properties; electronic structures; n-type conducting polymers; electron affinity; redox properties.

15. NUMBER OF PAGES
36

16. PRICE CODE

17. SECURITY CLASSIFICATION OF REPORT	18. SECURITY CLASSIFICATION OF THIS PAGE	19. SECURITY CLASSIFICATION OF ABSTRACT	20. LIMITATION OF ABSTRACT
Unclassified	Unclassified	Unclassified	Unlimited

OFFICE OF NAVAL RESEARCH

GRANT N00014-94-1-0540

R&T Code 3132111

Kenneth J. Wynne

Technical Report No. 16

Electrochemical Properties and Electronic Structures of Conjugated Polyquinolines and Polyanthrazolines

by

Ashwini K. Agrawal and Samson A. Jenekhe

Published

in

Chemistry of Materials

University of Rochester
Department of Chemical Engineering
Rochester, NY

September 9, 1996

TECHNICAL REPORT DISTRIBUTION LIST - GENERAL

Office of Naval Research (1)*
Chemistry and Physics Division
Ballston Tower 1, Room 503
800 North Quincy Street
Arlington, Virginia 22217-5660

Defense Technical Information Center (2)
Building 5, Cameron Station
Alexandria, VA 22314

Dr. James S. Murday (1)
Chemistry Division, Code 6100
Naval Research Laboratory
Washington, D.C. 20375-5000

Dr. Kelvin Higa (1)
Chemistry Division, Code 385
Naval Air Weapons Center
Weapons Division
China Lake, CA 93555-6001

Dr. Peter Seligman (1)
Naval Command, Control and
Ocean Surveillance Center
RDT&E Division
San Diego, CA 92152-5000

Dr. Richard W. Drisko (1)
Naval Civil Engineering
Laboratory
Code L52
Port Hueneme, CA 93043

Dr. Harold H. Singerman (1)
Naval Surface Warfare Center
Carderock Division Detachment
Annapolis, MD 21402-1198

Dr. Eugene C. Fischer (1)
Code 2840
Naval Surface Warfare Center
Carderock Division Detachment
Annapolis, MD 21402-1198

* Number of copies to forward

Electrochemical Properties and Electronic Structures of Conjugated Polyquinolines and Polyanthrazolines

Ashwini K. Agrawal and Samson A. Jenekhe*
Department of Chemical Engineering and Center for Photoinduced Charge Transfer
University of Rochester, Rochester, New York 14627-0166

ABSTRACT

The effects of molecular structure on the electronic structure and redox properties of a series of 22 systematically designed conjugated polyquinolines and polyanthrazolines are explored by cyclic voltammetry and spectroelectrochemistry on thin films. The measured electrochemical bandgap of the series of conjugated polymers was in the range 2.0-3.1 eV and found to be in good agreement with the optical bandgap. The oxidation and reduction potentials, ionization potential, and electron affinity of the series of polymers were correlated with their main structural features. All the polyquinolines and polyanthrazolines had reversible reduction with formal potentials of -1.57 to -2.08 V (versus SCE) which make them excellent n-type semiconducting polymers. Polymers containing anthrazoline units have a higher electron affinity by 0.3-0.4 eV than those containing bis(quinoline) units. On the other hand, thiophene-linked polymers have a lower ionization potential by 0.45-0.5 eV than those with phenylene linkages. Thus, thiophene-linked polyanthrazolines combine both low ionization potentials (~4.8-4.9 eV) and high electron affinities (~2.9 eV) and as a result can be p-type and n-type doped to conducting polymers with relatively more stability in air. Spectroelectrochemistry of the thiophene-linked polymers revealed features characteristic of polarons and bipolarons or radical ion dimers. The results suggest that the series of polyquinolines and polyanthrazolines are promising electronic and optoelectronic materials.

INTRODUCTION

Conjugated polymers that combine enhanced electronic, optoelectronic, or nonlinear optical properties with excellent mechanical properties, high thermal stability, and good processability are the subject of much current research effort.[1] One such class of conjugated polymers which has attracted our attention is the rigid-rod polyquinolines and polyanthrazolines. This class of polymers has excellent mechanical strength,[2,3] high thermal stability,[3] and can be processed into thin films and fibers using the approach of soluble coordination complexes in organic solvents.[4] We have extensively investigated the linear optical properties (optical absorption spectra, optical losses, dispersion of refractive index, etc.),[4] third-order nonlinear optical properties,[5] and photoconductivity[6] of the conjugated polyquinolines and have found them to be very interesting and promising materials. However, in order to further improve the electronic, optoelectronic, and nonlinear optical properties of this class of polymers and establish the underlying structure-property relationships, we have synthesized a systematically designed series of new polyquinolines and polyanthrazolines.[7]

We have found that all the conjugated polyquinolines reported in the literature prior to our studies have large bandgaps (~2.8 eV)[4] and only moderate electrical conductivity (10^{-3} to 10 S/cm) on *n-type* doping.[8] The *n-type* doped polymers were found to be highly sensitive to ambient conditions and unstable in air. Also, *p-type* doping was difficult to achieve by either chemical or electrochemical methods.[8] Theoretical calculations on the basic polyquinoline, poly(2,6-(4-phenyl quinoline)) (PPQ), showed a high ionization potential, a large electron affinity, and small bandwidths.[9] Therefore, in order to improve the electronic structure and properties of the polyquinolines, we have modified their conjugated backbone in a very systematic way. Steric hindrances between the various segments of the polymer backbone were reduced or eliminated by introducing conjugated spacers or by fusing the segments together.[4] In another approach,[7] replacement of the phenylene moieties in the phenylene-linked polyquinolines with thiophene moieties was shown to have substantial and beneficial effect on the electronic and optical properties

of the polymers. Compared to the phenylene-linked polyquinolines, the corresponding thiophene-linked polyquinolines were found to exhibit a dramatic red shift of the optical absorption spectra, a reduction in the optical bandgap by 0.3-0.5 eV, and a significant increase of the oscillator strength of the lowest energy optical absorption. Thus, bithiophene-linked polyquinolines and polyanthrazolines that combine bandgaps of as small as 2.0 eV with good mechanical and thermal properties were realized.[7]

In this paper, we report the results of studies exploring the effects of molecular structure on the electronic structure and redox properties of a series of π-conjugated polyquinolines and polyanthrazolines by cyclic voltammetry and spectroelectrochemistry on thin films. The molecular structures of the conjugated polymers investigated in the present study are shown in Charts I, II, and III. To facilitate elucidation of the effects of molecular structure on the electronic structure and redox properties, the structural features of the 22 polymers in Charts I, II, and III can be classified into five groups: phenylene-linked polyquinolines; phenylene-linked polyanthrazolines; thiophene-linked polyquinolines; thiophene-linked polyanthrazolines; and thiophene-linked polyquinolines with donor or acceptor side groups. The synthesis and characterization,[7] thin film processing, [4] and nonlinear optical properties[5] of these polymers have been reported previously.

EXPERIMENTAL SECTION

The detailed synthesis, purification, and characterization of the polymers is described elsewhere.[7] All of the materials were well characterized for their chemical structure and other physical properties.

Acetonitrile (ultrapure, 99+%, 0.01-0.03% water content) was obtained from Johnson Matthey Electronics and was used as received. Tetrabutylammonium hexaflurophosphate ($TBAPF_6$) was obtained from Aldrich. For cyclic voltammetry, an electrolyte solution of 0.1M $TBAPF_6$ in acetonitrile was used in all experiments. All solutions in the cell were purged with

ultrahigh purity N_2 for 10-15 min before each experiment and a blanket of N_2 was used during the experiment. Platinum wire electrodes were used as both counter and working electrodes and silver/silver ion (Ag in 0.1M $AgNO_3$ solution, from Bioanalytical Systems, Inc.) was used as a reference electrode. The Ag/Ag^+ ($AgNO_3$) reference electrode was calibrated at the beginning of the experiments every day by running cyclic voltammetry on ferrocene as the internal standard in an identical cell without any polymer on the working electrode. The potential values obtained in reference to Ag/Ag^+ electrode were converted in reference to internal standard of ferrocenium/ferrocene (Fc^+/Fc). The polymers were coated onto the working electrode by dipping the Pt wire electrode in the viscous polymer solutions. The polymer solutions were made in 15-20 wt% di-m-cresyl phosphate (DCP)/m-cresol. The coated electrode was dried in a vacuum oven at 90 °C resulting in a thin film of polymer-DCP complex on the Pt electrode. To obtain the pure polymer coatings on the electrode, the polymer-DCP complex on the Pt wire was treated in 10 % (v/v) triethylamine in ethanol for 24 h and then dried in a vacuum oven at 70-80 °C. This procedure gave a thin film of the pure polymer coated onto the platinum electrode for the electrochemical experiments.[4] Thin films of dried polymer-DCP complexes on Pt wire electrodes were also used directly for some of the electrochemical experiments. In such cases, the electrode bound polymer-DCP complex was electrochemically converted to the pure polymer before proceeding with the reduction or oxidation cycles. This conversion was carried out by continuously scanning the polymer-DCP complex on Pt working electrode in the voltage range of -0.3 to -1.4 V vs. SCE for 3-4 cycles. The electrochemical equipment used for the experiments was an EG&G Princeton Applied Research Potentiostat/Galvanostat Model 270/with option board 96. Data were collected and analyzed using Electrochemical Analysis System Software for Model 270 on a IBM PS/2 model 50 computer. It was found that the peak current of the cyclic voltammograms (CVs) increased with increasing scan rate in the 1-100 mV/s range but the shape and positions of the CVs were similar at the various scan rates. Therefore, a scan rate of 20 mV/s was used in obtaining all the cyclic voltammograms (CVs) reported here.

The potential values obtained versus Fc^+/Fc were converted to versus saturated calomel

electrode (SCE) by adding a constant of 0.1588 V to them. The conversion is based on the following known reduction potentials from the literature.[10,11] The reduction potential of ferrocenium versus NHE (normal hydrogen electrode) is 0.4 V and the reduction potential of SCE versus NHE is 0.2412 V. Therefore, the reduction potential of ferrocenium versus SCE is 0.1588 V. The solid state ionization potential (IP) and electron affinity (EA) of the polymers were estimated by using following relations:[12] $[E_{onset}]^{ox} = IP - 4.4$ and $[E_{onset}]^{red} = EA - 4.4$, where $[E_{onset}]^{ox}$ and $[E_{onset}]^{red}$ are the onset potentials for the oxidation and reduction of polymers versus SCE. These empirical relations were obtained by fitting valence effective Hamiltonian (VEH) calculations to the corresponding experimental data.[12] The onset potentials were determined from the intersection of two tangents drawn at the rising current and background charging current of a cyclic voltammogram.

Spectroelectrochemistry experiments were carried out in a two compartment glass cell with an ITO (indium tin oxide) coated glass working electrode, a platinum wire counter electrode in the first compartment, and a reference $Ag/AgNO_3$ electrode in the second compartment, which is separated from the first compartment by a fine glass frit. Thin films (less than 1μm) of the polymers were deposited on ITO-coated glass using techniques described elsewhere.[4] The cell was placed in the path of the sample light beam in a Perkin Elmer UV/vis/NIR spectrophotometer (Model Lambda 9) and a spectrum was taken at various potentials by taking a 0.05 to 0.1 V potential steps. After each potential step, the current in electrochemical system was allowed to come to an equilibrium (~20 minutes) before taking the optical absorption spectrum. The absorption spectrum for background correction was obtained by taking a UV/vis/NIR spectrum of a blank cell (electrochemical cell with ITO-coated glass working electrode but without the polymer coating) with identical conditions and parameters as the polymer experiment.

Thick (~2-4 μm) polymer films were used for conductivity measurements and were doped using a similar experimental setup as described above. Thick films for conductivity measurements, which were deposited on ITO-coated glass for the electrochemical doping cycle, were rinsed with

acetonitrile after doping, and then peeled off onto an adhesive tape. Once the films on the adhesive tape were dried in vacuum at room temperature, their conductivity was measured using a four point probe method or a two point probe method.

RESULTS AND DISCUSSION

Electrochemical Regeneration of Pure Polymers.

Since the polymer thin films on Pt electrodes were prepared from the soluble DCP complex and chemical regeneration in 10% (v/v) triethylamine in ethanol, it was essential to establish an electrochemical criterion of purity of the polymer thin films. Regeneration or conversion of the polymer-DCP complex to the pure polymer films on Pt electrode was therefore characterized by cyclic voltammetry. A vacuum dried DCP-polymer complex on the platinum working electrode was cycled repeatedly between -0.5 V to -1.5 V (versus Fc^+/Fc) in order to regenerate the polymer to its pure form. A small anodic current with a peak between -1.2 to -1.4 V versus Fc^+/Fc, characteristic of the regeneration process, was observed in the first cycle. With every subsequent cycle as the polymer regenerated, the current was substantially reduced. After running the polymer through four to five regeneration cycles, only a very small residual current was observed in the potential range -0.5 to -1.5 V. Figure 1A shows typical cyclic voltammograms for the regeneration of a PBTPQ-DCP complex in three cycles between -0.35 to -1.35 V (vs SCE). In Figure 1B is shown the fourth cycle along with the three previous cycles of Figure 1A indicating the complete disappearance of the anodic current due to the complex and observation of a reversible reduction of the pure PBTPQ film. For comparison, the cyclic voltammogram (CV) of a PBTPQ film which was *chemically* regenerated by treatment of the PBTPQ-DCP coated Pt electrode in Et_3N/ethanol was obtained and found to be identical to the CV in Figure 1B. In general, the oxidation and reduction potentials as well as other electrochemical characteristics of polyquinoline films *electrochemically* regenerated were found to be identical to those obtained on *chemically*

regenerated polymer films. Also, the optical absorption spectra of electrochemically regenerated polymer films on ITO-coated glass were found to be identical to those of the corresponding chemically regenerated polymer films. These results confirm the purity of the polymer films prepared from their soluble DCP complexes and provide an electrochemical means of following the decomplexation or regeneration process. All the redox properties of the polyquinolines and polyanthrazolines reported in subsequent sections were determined on the polymer films prepared by chemical regeneration.

Redox Properties

The reduction and oxidation (redox) potentials of all the 22 polyquinolines and polyanthrazolines shown in Charts I, II, and III were determined by cyclic voltammetry. To facilitate a discussion of the effects of molecular structure on the redox properties we first examine the basic polyquinoline **1** (PPQ). Figure 2 shows the cyclic voltammogram (CV) of PPQ from which we obtain a formal reduction potential ($E^{0\prime}$) of -1.89 V versus SCE. The reduction potential of this polymer has been reported in the literature[13] as -1.65 V (vs. SCE), which is different from our result. The origin for this difference is not clear due to the lack of details in the prior CV characterization of this polymer. We believe that the present value of the reduction potential of PPQ is accurate.

Figure 3 shows the cyclic voltammograms of the oxidation of PBPQ (**2b**) and PBDA (**3b**) and Figure 4 shows the CVs of the corresponding reduction of the same polymers. As can be seen from these figures, the reduction potential ($E^{0\prime}$) of the *anthrazoline*-containing polymer PBDA is significantly higher (-1.66 V vs. SCE) than that of the *bis(quinoline)*-containing PBPQ (-2.0 V vs. SCE), whereas the oxidation potential (E_{pa}) of PBDA (1.15 V) shows only a small decrease compared to PBPQ (1.23 V). Reduction (n-type doping) of both polymers shows excellent reversibility as evident in Figure 4. Under inert atmosphere, the polymers were repeatedly doped and dedoped without any noticeable changes in the characteristic of their reduction CVs. However, the oxidation (p-type doping) of both PBPQ and PBDA were irreversible (Figure 3), and the

oxidation potentials were found to shift to higher values with every subsequent doping-dedoping cycle. Clearly, the most profound effect of the structure on redox properties in going from the bis(quinoline) polymers **2** (Chart I) to anthrazoline polymers **3** (Chart I) is the significant increase of the reduction potential and slight decrease of the oxidation potential. This general conclusion and comparison hold for the other members of the polyquinolines **2** and polyanthrazolines **3** whose redox potentials are collected in Table 1.

In Figures 5 and 6, respectively, the reduction and oxidation CVs of thiophene-linked polyquinoline PBTPQ (**2g**) are compared with those of biphenyldiyl-linked polyquinoline PBPQ (**2b**). Although, there is a moderate increase of the reduction potential ($E^{0\prime}$) of PBTPQ (-1.85 V vs. SCE) compared to that of PBPQ (-2.0 V), the characteristics of the reduction (n-type doping), such as reversibility and repeatability, do not change in going from the biphenyldiyl-linked polyquinoline PBPQ to the bithienydiyl-linked polyquinoline PBTPQ (Figure 5). However, there is a dramatic improvement in the characteristics of the oxidation of PBTPQ compared to those of PBPQ (Figure 6). Not only has the oxidation potential of PBTPQ be shifted to a substantially lower potential compared to PBPQ, the p-type doping is more reversible, and PBTPQ can be repeatedly doped-dedoped for many cycles without significant changes in its oxidation peak characteristics. These characteristics, i.e. low oxidation potential and relatively more reversible oxidation, were observed in all the thiophene-linked polyquinolines. Similarly, in contrast to phenylene-linked polyanthrazolines, thiophene-linked polyanthrazolines showed significantly lower oxidation potentials (Table 1), more reversibility of the oxidation (p-type doping), and stability over many doping and dedoping cycles. One such example of thiophene-linked polyanthrazolines in comparison to phenylene-linked polyanthrazolines is shown in Figures 7 and 8. Figure 7 shows the oxidation CV of PBTDA in comparison to that of PBDA, and Figure 8 shows their reduction CVs. The reduction potential and peak characteristics of the two polymers PBTDA and PBDA remained relatively similar to each other, whereas the oxidation potential of PBTDA (**3g**) is significantly reduced relative to PBDA (**3b**). The most important conclusion from these results on the effects of the linking R group on the redox properties of the polyquinolines and

polyanthrazolines is that the thiophene-based spacers significantly reduce the oxidation potential and dramatically improve the reversibility of the oxidation of this class of conjugated polymers.

The effect of electron donating (-OCH_3) and electron withdrawing (-F) side groups on the redox properties of the polyquinolines was explored with the bithienyldiyl-linked polymers in Chart III, **4a**, **4b**, and **4c**. These thiophene-linked polyquinolines with donor or acceptor side groups did not exhibit reversibility of their oxidation in contrast to the other thiophene-linked polymers (Chart II). However, their reduction CVs were reversible and were stable to repeated doping-dedoping cycles. The effects of electron donating and electron accepting groups on the oxidation and reduction potentials of the polymers were found to be weak as shown in Table 1. These results suggest that the redox properties of this class of conjugated polymers are determined primarily by the backbone structure in accord with our prior UV-Vis spectra.[7]

Electronic Structure

The electronic structure of the conjugated polyquinolines and polyanthrazolines and the effects of systematic changes in the molecular structure of the polymers have been determined from the redox properties. The solid state ionization potential (IP) and electron affinity (EA) of each polymer were obtained from the onset oxidation and reduction potentials.[12] Table 2 lists the solid state IP and EA values for the series of polyquinolines and polyanthrazolines. Also included in Table 2 are the electrochemical bandgap (E_g^{el}) and optical bandgap (E_g^{opt})[4,7] of the same polymers.

The experimentally measured IP value of the basic polyquinoline PPQ (5.35 eV) was found to be 12% smaller than the theoretically calculated[9] value of 6.0 eV. The measured electron affinity value of 2.62 eV is also to be compared to the calculated value of 2.8 eV for PPQ. Whereas there was an excellent agreement (within 3%) between the values of the bandgap of PPQ determined by electrochemical (2.73 eV) and optical (2.65 eV) methods, the theoretically calculated bandgap (E_g = 3.1 eV) was much higher. These results are in contrast to the remarkable

agreements often reported between the VEH calculated IP and E_g values and those determined electrochemically.[12,14] However, our experimental results as well as the theoretical calculations[9] are qualitatively correct in explaining the doping characteristics of PPQ and some of its phenylene derivatives (PBPQ, PSPQ, etc.) which are clearly better n-type materials than p-type.

The measured electrochemical bandgap (E_g^{el}) and optical bandgap (E_g^{opt})[4,7] of the series of 22 polyquinolines and polyanthrazolines (Table 2) were in excellent agreement, generally less than 3% difference, except in some cases where the difference was 7-10%. The E_g^{el} values for all the polymers were in the range of 2.03 eV to 3.08 eV. The trends in the E_g^{el} values with polymer structure were similar to those observed for the optical bandgap[4,7] among the five groups within the 22 members of the polyquinolines and polyanthrazolines: (a) phenylene-linked polyquinolines; (b) phenylene-linked polyanthrazolines; (c) thiophene-linked polyquinolines; (d) thiophene-linked polyanthrazolines; (e) thiophene-linked polyquinolines with donor or acceptor side groups. Although there was only a small difference in the E_g^{el} values within each of these five subgroups, there was a major change in the bandgap as one moves from one subgroup to another. In accord with previous optical absorption results (E_g^{opt}), thiophene-linked polyanthrazolines have the smallest bandgap of about 2.0 eV.

From the ionization potentials and electron affinities of the polymers listed in Table 2, some very clear and specific trends among the polymers of the five subgroups can be derived. Among polymers with structure **2** and **3** (Charts I and II) and identical linking R segment, the ionization potential decreases by only a small value of 0.1-0.15 eV in going from phenylene-linked polyquinolines to phenylene-linked polyanthrazolines and decreases only negligibly in going from thiophene-linked polyquinolines to thiophene-linked polyanthrazolines. However, the electron affinity of all the polyanthrazolines which contain the three fused ring anthrazoline unit is substantially higher than that of the polyquinolines containing bis(quinoline) unit by about 0.3-0.4 eV. A similar comparison between polymers with structure **2** (polyquinolines) and structure **3** (polyanthrazolines) in which the linking R-moiety is varied shows different results. For example,

when a phenylene linkage in polyquinolines is replaced by a thiophene linkage, the ionization potential of the polymers decreases significantly by about 0.45-0.5 eV and the electron affinity increases only moderately by about 0.15-0.20 eV. Similarly, when thiophene-linked polyanthrazolines are compared with phenylene-linked polyanthrazolines, a substantial decrease of the ionization potential by about 0.35 eV is seen in the thiophene-linked polyanthrazolines. However, the electron affinity, as in the case of the polyquinolines, increases by only a small value (0.05-0.08 eV).

The above results suggest that a fused ring anthrazoline structure in place of a bis(quinoline) segment in a polymer has a profound effect on the position of the lowest unoccupied molecular orbitals (LUMO or π^*-band). Compared to the polyquinolines, the LUMO band in the polyanthrazolines is shifted to a significantly lower energy. However, this structural change has only a moderate effect on the position of the highest occupied molecular orbitals (HOMO or π-band). On the other hand, the replacement of phenylene linkages with thiophene linkages in both polyquinolines (**2**) and polyanthrazolines (**3**) has a much greater effect on the position of the HOMO than on the LUMO level. The HOMO of thiophene-linked polymers are pushed up to a significantly higher energy than that of phenylene-linked polymers whereas the position of the LUMO of thiophene-linked polymers did not change significantly from that of phenylene-linked polymers. Consequently, in thiophene-linked polyanthrazolines the HOMO is pushed up and at the same time the LUMO is pushed down in energy, i.e. there is a substantial decrease in the ionization potential and an increase in the electron affinity, in comparison to those of phenylene-linked polyquinolines. As an illustration, compared to the biphenylene-linked polyquinoline PBPQ, the bithiophene-linked polyanthrazoline PBTDA shows an overall decrease of the ionization potential by about 0.5 eV from ~5.5 eV to ~5 eV and an overall increase of the electron affinity by about 0.5 eV from 2.42 eV to 2.9 eV. This gives an overall reduction of the electrochemical bandgap by about 1 eV in PBTDA compared to PBPQ.

The electron donor and acceptor side groups in polymers **4** (Chart III) do not seem to have

any significant effect on the positions of the HOMO and LUMO of the thiophene-linked polyquinolines. These results are in agreement with the optical absorption spectra[7c] of these polymers which show little differences in the optical bandgaps of the three polyquinolines (**4a**, **4b**, **4c**).

The electronic structure and electrochemical properties of many conjugated polymers have been extensively investigated,[12,14] including the ionization potentials, electron affinity, and doping characteristics. The electrochemically determined parameters IP, EA, and E_g^{el} for some well known conducting polymers are shown in Table 3 along with our results for three polyquinolines (PPQ, PBPQ, and PBTVDA). As can be seen from Table 3, the ionization potential of PBTVDA (4.92 eV) is only slightly larger than that of polyacetylene and polythiophene vinylene (PTV) and is very close to that of polythiophene (PT) and poly(paraphenylene vinylene) (PPV). It is significantly smaller than that of polyparaphenylene (PPP), polydiacetylene, PPQ, and the phenylene-linked polyquinolines (for example PBPQ). This comparison suggests that the new thiophene-linked polyquinolines (Chart II), unlike phenylene-linked polyquinolines such as PBPQ and PSPQ in Chart I, could be readily oxidized using common p-type dopants, like iodine vapors, AsF_5, etc. Also, the electron affinity of the new polyanthrazolines (EA = ~2.9 eV) is quite large. Compared to the electron affinities of polypyrrole (PPY), PPP, PPV, PPQ, and PBPQ, it is substantially larger. It is also comparable to the EA values of polydiacetylene and PT, which suggests that the new polyquinolines are better candidates for n-type doping than the known phenylene-linked polyquinolines PBPQ and PSPQ.[8] Even though, having a low ionization potential and a large electron affinity in conjugated polymers are the necessary conditions for obtaining high electrical conductivity in the doped state, they are not sufficient. Theoretical calculations on PPQ have shown the bandwidth to be very small (0.5-0.7 eV), and therefore, have suggested limited mobility of the charge carriers. It is essential to calculate the HOMO and LUMO bandwidths of the new thiophene-linked polymers before their potential as better electrical conductors than phenylene-linked polyquinolines and other classes of conjugated polymers can be fully assessed. However, it is known that as the π-electron delocalization and conjugation along a

polymer backbone increases, the bandwidth of the polymer increases too.[12,14] Therefore, it is reasonable to expect that the new thiophene-linked polymers (Chart II) may show improved bandwidths and, hence, good electrical properties.

In general, the excellent reversibility of the reduction (or n-type doping) of all the polyquinolines and polyanthrazolines investigated, e.g. formal reduction potentials ($E^{0\prime}$) of -1.57 to -2.08 V (versus SCE) shown in Table 1, means that this class of conjugated polymers constitutes intrinsic n-type semiconducting polymers. Of the 22 polymers, only 8 with thiophene linkages exhibited quasi-reversible oxidation ($E^{0\prime}$ = 0.74 to 1.20 V(SCE), Table 1) which means that they also exhibit some p-type semiconducting properties. The remaining polymers have irreversible oxidation and hence poor p-type (hole transporting) properties. The polyquinolines and polyanthrazolines thus join aromatic *polyimines*[15] and *polybenzobisthiazoles*[16] as well-characterized n-type π-conjugated polymers. Recent advances in the electronic and optoelectronic applications of semiconducting polymers suggest the need of *n-type* (electron transporting) as well as *p-type* (hole transporting) materials.[17]

Spectroelectrochemistry and Doping Studies.

Preliminary spectroelectrochemical doping study of two thiophene-linked polyquinolines PBTPQ (**2g**) and PBTDA (**3g**) was done to shed light on the dopability of the new polymers and the nature of the charges produced by doping. Each of the polymers was coated onto an ITO-coated glass and optical absorption spectra were obtained *in situ* while the polymer film was being doped electrochemically. Figure 9 shows the optical absorption spectra of PBTDA at different potentials during oxidation. In the neutral state, PBTDA shows a red color and its optical absorption is given by spectrum 1 of Figure 9. In the doped state of PBTDA (spectra 2-6), three subbandgap features appearing at 675 nm (1.84 eV), 830 nm (1.50 eV), and >1600 nm (< 0.78 eV) can be observed. The oscillator strength of these bands, especially the one at 675 nm, increases with increasing oxidation level (or oxidation potential) at the expense of the oscillator

strength of the lowest energy transition (520 nm) of the pure polymer. Also, the peaks at 520 nm (λ_{max} of PBTDA), 675 nm, and 830 nm shift toward the higher energy with increasing level of doping. These results indicate the formation of subbandgap species. At low doping levels (spectra 2-6), the three absorption bands indicate the creation of stable polarons[12] as illustrated in the band structure diagram of Figure 10A. One of the two polaron states appears at 0.34 eV below the conduction band and the other 0.34 eV above the valence band. At higher oxidation potentials, a new peak at 620 nm evolves, and the peaks at 675 nm and 850 nm start disappearing (Figure 9, spectra 7-9). Also, the isosbestic points start to shift. Although, definite features are not discernible at this stage of doping, the multiple absorption peaks and moving isosbestic points indicate the coexistence of more than one type of charged species in the doped polymer, possibly both polarons and bipolarons[12,18] or both polarons and radical ion-pair π-dimers.[19,20] Interchain or intrachain polaron pairs (radical ion dimers) are expected to be spinless like bipolarons.[19,20]

Similar features are seen in the *in situ* optical absorption spectra during the oxidation of PBTPQ (Figure 11), which again supports the formation of polarons at the initial levels of doping (at low potentials) of PBTPQ. At higher potentials, as in the case of PBTDA, multiple absorption peaks and a moving isosbestic point are visible. Figure 10B illustrates the band structure of p-type doped PBTPQ at low doping level. Figure 12 shows the optical absorption spectra of n-type doping (reduction) of PBTPQ at different reduction potentials. Spectrum 1 in Figure 12 is the optical absorption of the pure PBTPQ. In the doped state, even at very low levels of doping (spectra 2 and 3), PBTPQ shows only two subbandgap absorptions at 725 nm (1.71 eV) and >1600 nm (< 0.78 eV). The oscillator strength of these subbandgap absorptions increases with increasing doping level (or decreasing potential) whereas the lowest energy absorption band (468 nm) of the pure polymer decreases (spectrum 4). These features indicate the formation of bipolarons[12,18] or π-dimers[19,20] in the n-type doped PBTPQ. The signatures of polarons, i.e. three absorption bands below the bandgap, were not observed at any time during the n-type doping of PBTPQ. It is possible that polarons in n-type doped PBTPQ are relatively unstable and they

combine to form bipolarons[12,18] or π-dimers (or polaron pairs)[19,20] after they are generated in the polymer. This feature of n-type doping of PBTPQ is in contrast to its p-type doping, where the polarons are relatively more stable. Figure 10C shows the bipolaron states in the band structure of PBTPQ. However, in order to unambiguously determine the nature of the charged species in the doped state of these polymers, further investigations are warranted. Towards this end, our future studies will include *in situ* ESR spectroscopy of electrochemically doped polyquinolines.

Several micrometers thick films of the thiophene-linked polymers, PBTPQ and PBTDA, were cast onto ITO glass electrodes and were doped electrochemically in the same electrolyte as was used in the spectroelectrochemistry experiments. On doping the polymers, they turned to bluish black or brownish black color from the dark orange (PBTPQ) or red (PBTDA) color of their neutral forms. After doping, the films were removed from the cell in air, rinsed with acetonitrile, and then dried in vacuum at room temperature (30 °C, 1-2 hr). Interestingly, the doped films of thiophene-linked polymers upon exposure to air, unlike the phenylene-linked polyquinolines which dedopes within few seconds, did not show any noticeable change from their doped state. The conductivity (~10^{-3} S/cm) of the n-type or p-type doped samples remained intact for over 2-3 days before dropping by 2 orders of magnitude over a period of 2 weeks. Further studies on doping, conductivity, and charge transport of the polyquinolines are underway and will be reported in the future.

CONCLUSIONS

A series of conjugated polymers in the class of polyquinolines and polyanthrazolines have been investigated by cyclic voltammetry in order to explore the effects of molecular structure on the electronic structure and redox properties of π-conjugated polymers. A close agreement was found between the bandgaps determined electrochemically (E_g^{el}) and those determined from the threshold of the optical absorption (E_g^{opt}) of the polymers. Ionization potential (IP) and electron affinity (EA) of the polymers were correlated with the main structural features of this class of polymers.

Polymers containing anthrazoline units (polyanthrazolines) were found to have higher electron affinity by 0.3-0.4 eV than those with bis(quinoline) unit (polyquinolines). On the other hand, polymers containing thiophene linkages showed significantly lower ionization potentials by 0.45-0.5 eV than those with phenylene linkages. Thus, new polymers such as PBTDA, PBTADA, and PBTVDA, with both anthrazoline unit and thiophene linkages showed a combined effect of the two features: low ionization potentials (~4.8-4.9 eV) and high electron affinities (~2.9 eV). Unlike the phenylene-linked polymers, the thiophene-linked polymers showed improved reversible p-type doping, and the doped polymers were found to be relatively more stable in air.

Spectroelectrochemistry of two thiophene-linked polymers, PBTPQ and PBTDA, exhibited absorption bands below the bandgap of the neutral polymers which suggest polaron and bipolaron species in the doped polymers. At low levels of p-type doping of PBTPQ, relatively stable polarons were generated in contrast to the n-type doping of PBTPQ where only features characteristic of either bipolarons or π-dimers were observed. The new thiophene-linked polyquinolines and polyanthrazolines are promising electronic and optoelectronic materials with intrinsic electronic properties comparable to or better than many other conjugated polymers.

ACKNOWLEDGEMENTS

This research was supported by the National Science Foundation (CTS-9311741, CHE-9120001) and Office of Naval Research.

REFERENCES

1. (a) Jenekhe, S. A., Ed. *Macromolecular Host-Guest Complexes: Optical, Optoelectronic, and Photorefractive Properties and Applications*, Materials Research Society Proceedings vol. 277, **1992** (Materials Research Society, Pittsburgh). (b) Bredas, J. L., Chance, R. R., Eds. *Conjugated Polymeric Materials: Opportunity in Electronics, Optoelectronics, and Molecular Electronics*, Kluwer Academic Publishers: Dordrecht, Holland, 1990. (c) Marder, S. R.; Sohn, J. E.; Stucky, G. D., Eds. *Materials for Nonlinear Optics: Chemical Perspectives*, American Chemical Society: Washington, DC, 1991.

2. (a) Wrasidlo, W.; Norris, S. O.; Wolfe, J. F.; Katto, T.; Stille, J. K. *Macromolecules* **1976**, *9*, 512-516. (b) Wrasidlo, W; Stille, J. K. *Macromolecules* **1976**, *9*, 505-511.

3. Stille, J. K. *Macromolecules* **1981**, *14*, 870-880.

4. Agrawal, A. K.; Jenekhe, S. A. *Chem. Mater.* **1992**, *4*, 95-104.

5. (a)Agrawal, A. K.; Jenekhe, S. A.; Vanherzeele, H; Meth, J. S. *J. Phys. Chem.* **1992**, *96*, 2837-2843. (b) Agrawal, A. K.; Jenekhe, S. A.; Vanherzeele, H; Meth, J. S.*Chem. Mater.* **1991**, *3*, 765-768. (c) Agrawal, A. K.; Jenekhe, S. A.; Vanherzeele, H; Meth, J. S. *Mater. res. soc. Proc.* **1992**, *247*, 253-258. (d) Agrawal, A. K.; Jenekhe, S. A.; Vanherzeele, H; Meth, J. S. *Polym. preprints (Am. Chem. Soc., Polym. Chem. Div.)* **1991**, *32(3)*, 124-125.

6. Abkowitz, M. A.; Stolka, M.; Antoniadis, H.; Agrawal, A. K.; Jenekhe, S. A *Solid State Commun.***1992**, *83*, 937-944.

7. (a) Agrawal, A. K.; Jenekhe, S. A. *Macromolecules* **1991**, *24*, 6806-6808. (b) Agrawal, A. K.; Jenekhe, S. A. *Macromolecules* **1993**, *26*, 895-905. (c) Agrawal, A. K.; Jenekhe, S. A. *Chem. Mater.* **1993**, *5*, 633-640. (d) Agrawal, A. K.; Jenekhe, S. A. *Polym.*

Preprint (Am. Chem. Soc., Polym. Chem. Div.) **1992**, *33(2)*, 349-350.

8. (a) Tunney, S. E.; Suenaga, J.; Stille, J. K. *Macromolecules* **1983**, *16*, 1398-1399; (b) Tunney , S. E.; Suenaga, J.; Stille, J. K. *Macromolecules* **1987**, *20*, 258-264.

9. Themans, B.; Andre, J. M.; Bredas, J. L. *Solid State Commun.* **1984**, *50*, 1047-1050.

10. *CRC Handbook of Chemistry and Physics*, CRC Press, Inc.: Boca Raton, Florida, USA, 68th Edition, p D151-D158.

11. Gagne, R. R.; Koval, C. A.; Lisensky, G. C. *Inorg. Chem.* **1980** *19*, 2855-2857.

12. (a) Bredas, J. L.; Silbey, R.; Boudreaux, D. S.; Chance, R. R. *J. Am. Chem. Soc.* **1983**, *105*, 6555. (b) Bredas, J. L. In: *Handbook of Conducting Polymers*, T. A. Skotheim, Ed. Marcel Dekker: New York, **1986**; pp 859-913. (c) Bredas, J. L.; Chance, R. R.; Baughman, R. H.; Silbey, R. *J. Chem. Phys.* **1982**, *76*, 3673. (d) Chance, R. R.; Boudreaux, D. S.; Bredas, J. L.; Silbey, R. In: *Polymers in Electronics* T. Davidson Ed.; ACS Symposium Series 242, Am. Chem. Soc.: Washington, DC, **1983**, 433-446. (e) Frommer J. E.; Chance, R. R. In: *Encyclopedia of Polymer Science and Engineering*, John Wiley & Sons, Inc.: New York, USA, Second Edition, **1986**, *5*, 462-507.

13. Deniscvich, P; Papir, Y. S.; Kurkov, V. P.; Current, S. P.; Schroeder, A. H.; Suzuki, S. *Polym. Prepr. (Am. Chem. soc., Div. Polym. Chem.)* **1983**, *24*, 330- 331.

14. (a) Eckhardt, H.; Jen, K. Y.; Shacklette, L. W.; Lefrant, S., in reference 1(b), pages 305-320. (b) Eckhardt, H.; Shacklette, L. W.; Jen, K. Y.; Elsenbaumer, R. L. *J. Chem. Phys.* **1989**, *91*, 1301-1315.

15. Yang, C.-J.; Jenekhe, S. A. *Macromolecules* **1995**, *28*, 1180-1196.

16. Osaheni, J. A.; Jenekhe, S. A. *Chem. Mater.* **1995**, *7*, 672-682.

17. Greenham, N. C.; Moratti, S. C.; Bradley, D. D. C.; Friend, R. H.; Holmes, A. B. *Nature* **1993**, *365*, 628-630.

18. Bredas, J. L.; Scott, J. C.; Yakushi, K.; Street, G. B. *Phys. Rev. B* **1984**, *30(2)*, 1023-1025.

19. (a) Hill, M. G.; Mann, K. R.; Miller, L. L.; Penneau, J.-F. *J. Am. Chem. Soc.* **1992**, *114*, 2728-2730. (b) Bäuerle, P.; Segelbacher, U.; Maier, A.; Mehring, M. *J. Am. Chem. Soc.* **1993**, *115*, 10217-10223.

20. Furukawa, Y. *Synth. Met.* **1995**, *69*, 629-632.

Table 1. Oxidation and Reduction potentials of polyquinolines and polyanthrazolines.

		Oxidation[a] (V)				Reduction[a] (V)			
	Polymer	E_{pa}	E_{pc}	$E^{0\prime}$	E_{onset}	E_{pa}	E_{pc}	$E^{0\prime}$	E_{onset}
1	PPQ	1.35	b	b	0.95	-2.0	-1.79	-1.89	-1.78
2a	PPPQ	1.30	b	b	1.07	-1.98	-1.87	-1.93	-1.9
2b	PBPQ	1.23	b	b	1.09	-2.07	-1.92	-2.0	-1.98
2c	PBAPQ	1.30	b	b	1.08	-2.03	-1.86	-1.94	-1.93
2d	PSPQ	1.14	b	b	0.95	-2.00	-1.92	-1.96	-1.92
2e	PDMPQ	1.32	b	b	1.04	-2.14	-2.02	-2.08	-2.04
3a	PPDA	1.21	b	b	0.87	-1.71	-1.54	-1.62	-1.57
3b	PBDA	1.15	b	b	0.94	-1.74	-1.58	-1.66	-1.54
3c	PBADA	1.15	b	b	0.96	-1.50	-1.72	-1.61	-1.51
3d	PSDA	1.10	b	b	0.87	-1.71	-1.59	-1.65	-1.59
3e	PDMDA	1.24	b	b	1.03	-1.74	-1.59	-1.66	-1.55
2f	PTPQ	1.21	1.18	1.20	0.87	-2.16	-1.70	-1.85	-1.84
2g	PBTPQ	0.93	0.85	0.89	0.64	-1.95	-1.76	-1.85	-1.84
2h	PBTAPQ	1.00	0.91	0.96	0.46	-1.81	-1.75	-1.78	-1.72
2i	PBTVPQ	0.85	0.75	0.80	0.51	-1.86	-1.69	-1.78	-1.77
3f	PTDA	1.09	1.00	1.04	0.66	-1.72	-1.51	-1.61	-1.53
3g	PBTDA	0.84	0.85	0.84	0.62	-1.72	-1.53	-1.62	-1.51
3h	PBTADA	0.74	0.73	0.74	0.54	-1.65	-1.58	-1.61	-1.43
3i	PBTVDA	0.96	0.80	0.88	0.52	-1.66	-1.49	-1.57	-1.51
4a	PBTPQA	0.84	b	b	0.62	-2.01	-1.82	-1.92	-1.95
4b	PBTPQA-F	0.83	b	b	0.61	-2.10	-1.76	-1.93	-1.98
4c	PBTPQA -OCH_3	0.84	b	b	0.57	-1.89	-1.83	-1.86	-1.76

E_{pc} = cathodic peak potential; E_{pa} = anodic peak potential;

$E^{0\prime} = (E_{pc} + E_{pa})/2$; E_{onset} = onset potential.

[a] All potential values are versus SCE.

[b] oxidation is not reversible under experimental conditions, therefore, potential values could not be determined.

Table 2. Electronic structure parameters of polyquinolines and polyanthrazolines.

	Polymer	[a]Ionization Potential (IP) (eV)	[b]Electron Affinity (EA) (eV)	[c]E_g^{el} (eV)	[d]E_g^{opt} (eV)
1	PPQ	5.35 [5.27][e]	2.62	2.73	2.65
2a	PPPQ	5.47 [5.28]	2.50	2.97	2.78
2b	PBPQ	5.49 [5.23]	2.42	3.07	2.81
2c	PBAPQ	5.48 [5.19]	2.47	3.01	2.72
2d	PSPQ	5.35 [5.13]	2.48	2.87	2.65
2e	PDMPQ	5.44 [5.37]	2.36	3.08	3.01
3a	PPDA	5.27 [5.30]	2.83	2.44	2.47
3b	PBDA	5.34 [5.42]	2.86	2.48	2.56
3c	PBADA	5.36 [5.46]	2.89	2.47	2.57
3d	PSDA	5.27 [5.27]	2.81	2.46	2.46
3e	PDMDA	5.43 [5.55]	2.85	2.58	2.70
2f	PTPQ	5.27 [5.05]	2.56	2.71	2.49
2g	PBTPQ	5.04 [4.89]	2.56	2.48	2.33
2h	PBTAPQ	4.86 [4.94]	2.68	2.18	2.26
2i	PBTVPQ	4.91 [4.86]	2.63	2.28	2.23
3f	PTDA	5.06 [5.04]	2.87	2.19	2.17
3g	PBTDA	5.02 [4.96]	2.89	2.13	2.07
3h	PBTADA	4.94 [4.97]	2.97	1.97	2.0
3i	PBTVDA	4.92 [4.89]	2.89	2.03	2.0
4a	PBTPQA	5.02 [4.81]	2.45	2.57	2.36
4b	PBTPQA-F	5.01 [4.75]	2.42	2.59	2.33
4c	PBTPQA $-OCH_3$	4.97 [5.00]	2.64	2.33	2.36

[a] determined from the onset oxidation potential.

[b] determined from the onset reduction potential.

[c] electrochemical bandgap $E_g^{el} = IP - EA$.

[d] optical bandgap E_g^{opt} from the optical absorption spectra [Ref. 4,7].

e determined from $IP = EA + E_g^{opt}$.

Table 3. Electrochemical properties of some conducting polymers.

Polymer	[a]IP (eV)	[b]EA (eV)	[c]E_g^{el} (eV)	Ref.
Polyacetylene	4.73	3.31	1.42	d,e
Polydiacetylene	5.2	3.1	2.1	d
Polythiophene	5.20	2.96	2.24	d,e
Polythiophene vinylene	4.76	---	---	e
Polyparaphenylene	5.42	2.58	2.84	d,e
Polyparaphenylene vinylene	5.11	2.71	2.40	e
Polypyrrole	4.0	1.0	3.0	d
PPQ	5.35	2.62	2.73	
PBPQ	5.49	2.42	3.07	
PBTVDA	4.92	2.89	2.03	

[a] values obtained from the onset oxidation potential of the polymer.
[b] obtained using: EA = IP - E_g, where IP and E_g are electrochemically determined values.
[c] electrochemical bandgap obtained using: E_g^{el} = IP - EA.
[d] reference 12 and references therein, [e] reference 14 and references therein.

Figure Captions.

Figure 1A. Cyclic voltammograms of PBTPQ-DCP complex indicating electrochemical regeneration.

Figure 1B Cyclic voltammogram at 20 mV/s scan rate of electrochemically regenerated PBTPQ film along with three regeneration CVs of Figure 1A. Curves 2 and 3 have essentially merged with the baseline.

Figure 2. Cyclic voltammogram of PPQ in 0.1M $TBAPF_6$ in acetonitrile at 20 mV/s scan rate.

Figure 3. Cyclic voltammogram of the oxidation of (a) PBPQ and (b) PBDA in 0.1M $TBAPF_6$ in acetonitrile at 20 mV/s scan rate.

Figure 4. Cyclic voltammogram of the reduction of (a) PBPQ and (b) PBDA in 0.1M $TBAPF_6$ in acetonitrile at 20 mV/s scan rate.

Figure 5. Cyclic voltammogram of the reduction of (a) PBPQ and (b) PBTPQ in 0.1M $TBAPF_6$ in acetonitrile at 20 mV/s scan rate.

Figure 6. Cyclic voltammogram of the oxidation of (a) PBPQ and (b) PBTPQ in 0.1M $TBAPF_6$ in acetonitrile at 20 mV/s scan rate.

Figure 7. Cyclic voltammogram of the oxidation of (a) PBDA and (b) PBTDA in 0.1M $TBAPF_6$ in acetonitrile at 20 mV/s scan rate.

Figure 8. Cyclic voltammogram of the reduction of (a) PBDA and (b) PBTDA in 0.1M $TBAPF_6$ in acetonitrile at 20 mV/s scan rate.

Figure 9. Optical absorption spectra of PBTDA taken *in situ* during electrochemical doping at different oxidation potentials.

Figure 10. Experimental energy level diagram of the band structure of: A, p-type doped PBTDA; B, p-type doped PBTPQ; C, n-type doped PBTPQ.

Figure 11. Optical absorption spectra of PBTPQ taken *in situ* during electrochemical doping at different oxidation potentials.

Figure 12. Optical absorption spectra of PBTPQ taken *in situ* during electrochemical doping at different reduction potentials.

Chart I

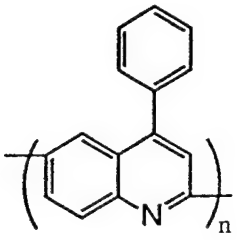

1

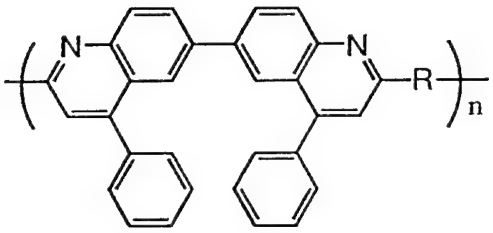

2

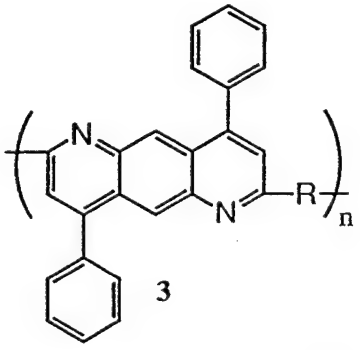

3

R

a

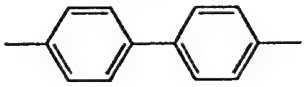

b

c

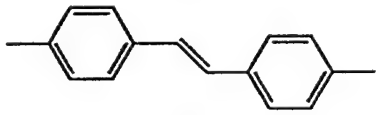

d

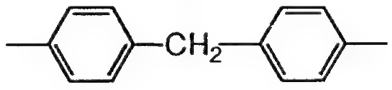

e

1	= PPQ		
2a	= PPPQ	3a	= PPDA
2b	= PBPQ	3b	= PBDA
2c	= PBAPQ	3c	= PBADA
2d	= PSPQ	3d	= PSDA
2e	= PDMPQ	3e	= PDMDA

Chart II

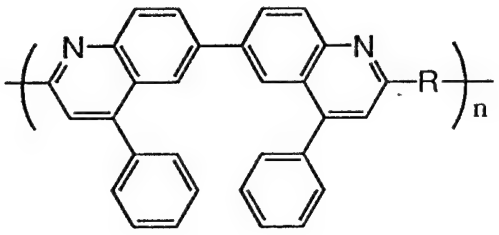

2

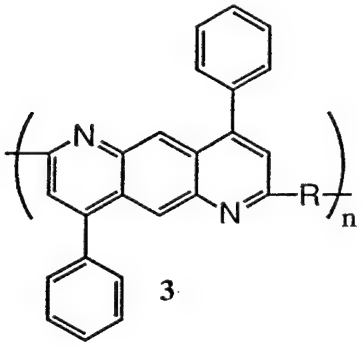

3

R

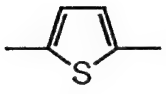

f

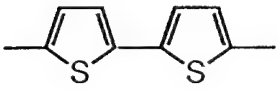

g

h

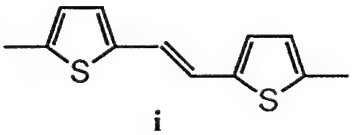

i

2f = PTPQ	3f = PTDA
2g = PBTPQ	3g = PBTDA
2h = PBTAPQ	3h = PBTADA
2i = PBTVPQ	3i = PBTVDA

Chart III

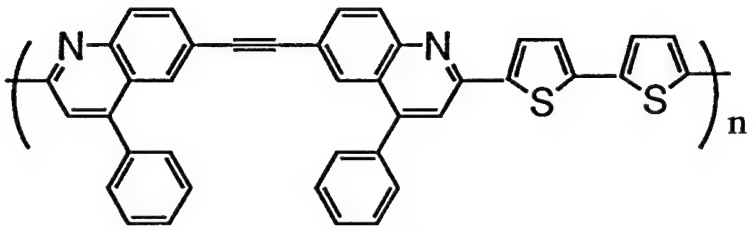

4a = PBTPQA

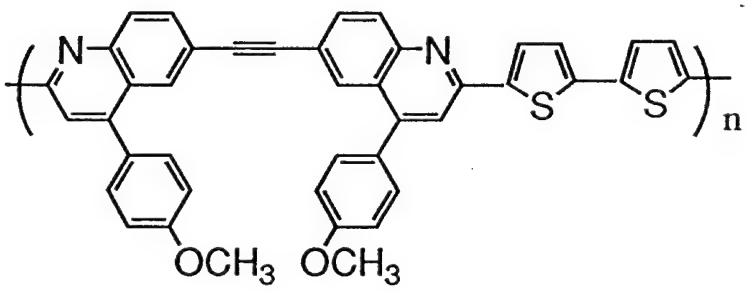

4b = PBTPQA-OCH_3

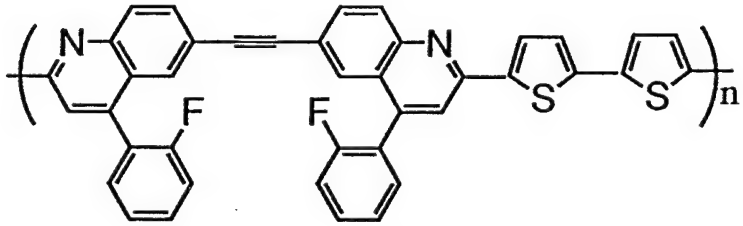

4c = PBTPQA-F

Figure 1A

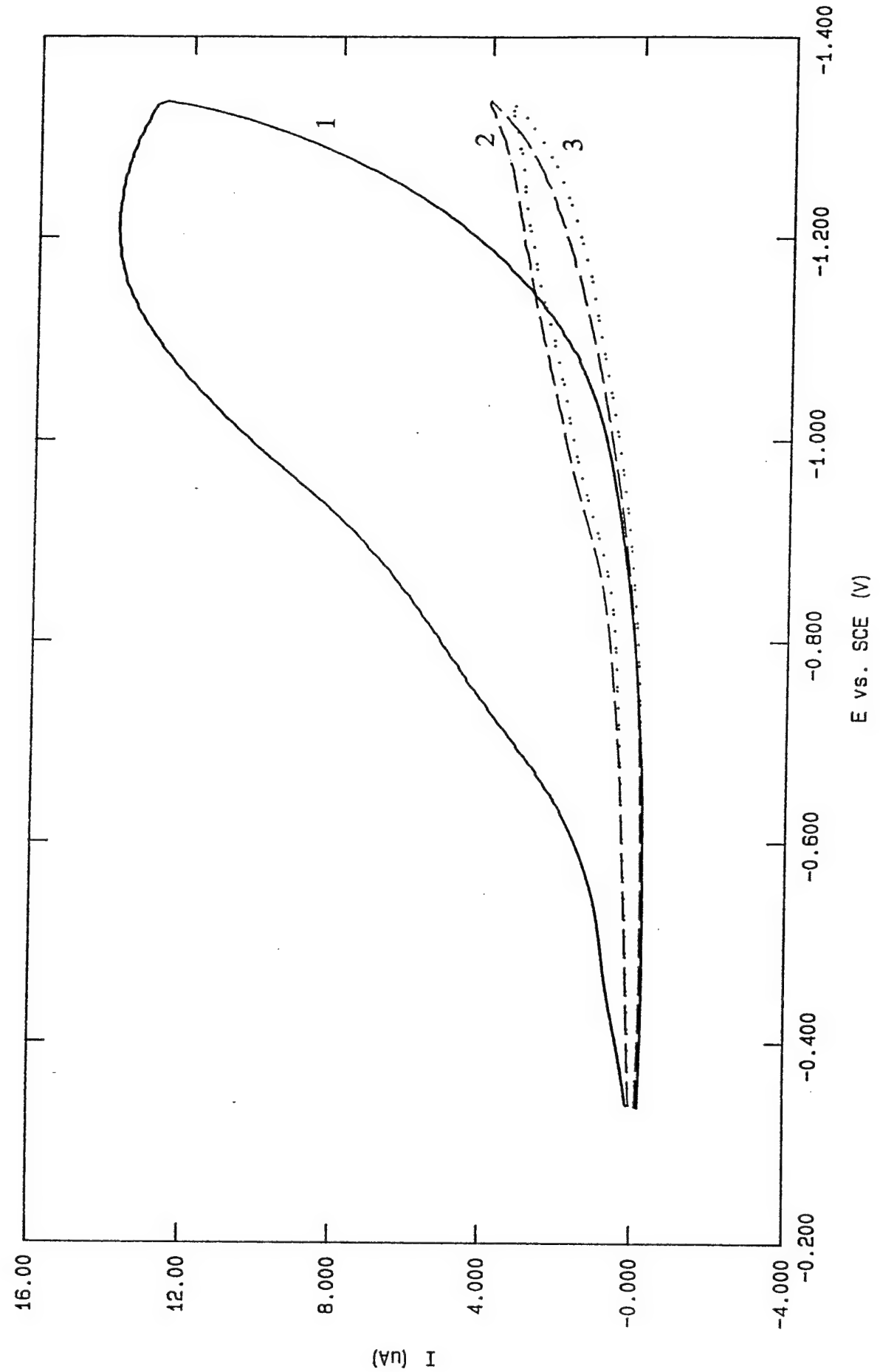
16.00
12.00
8.000
4.000
-0.000
-4.000
I (uA)
-0.200
-0.400
-0.600
-0.800
-1.000
-1.200
-1.400
E vs. SCE (V)
1
2
3

Figure 1B

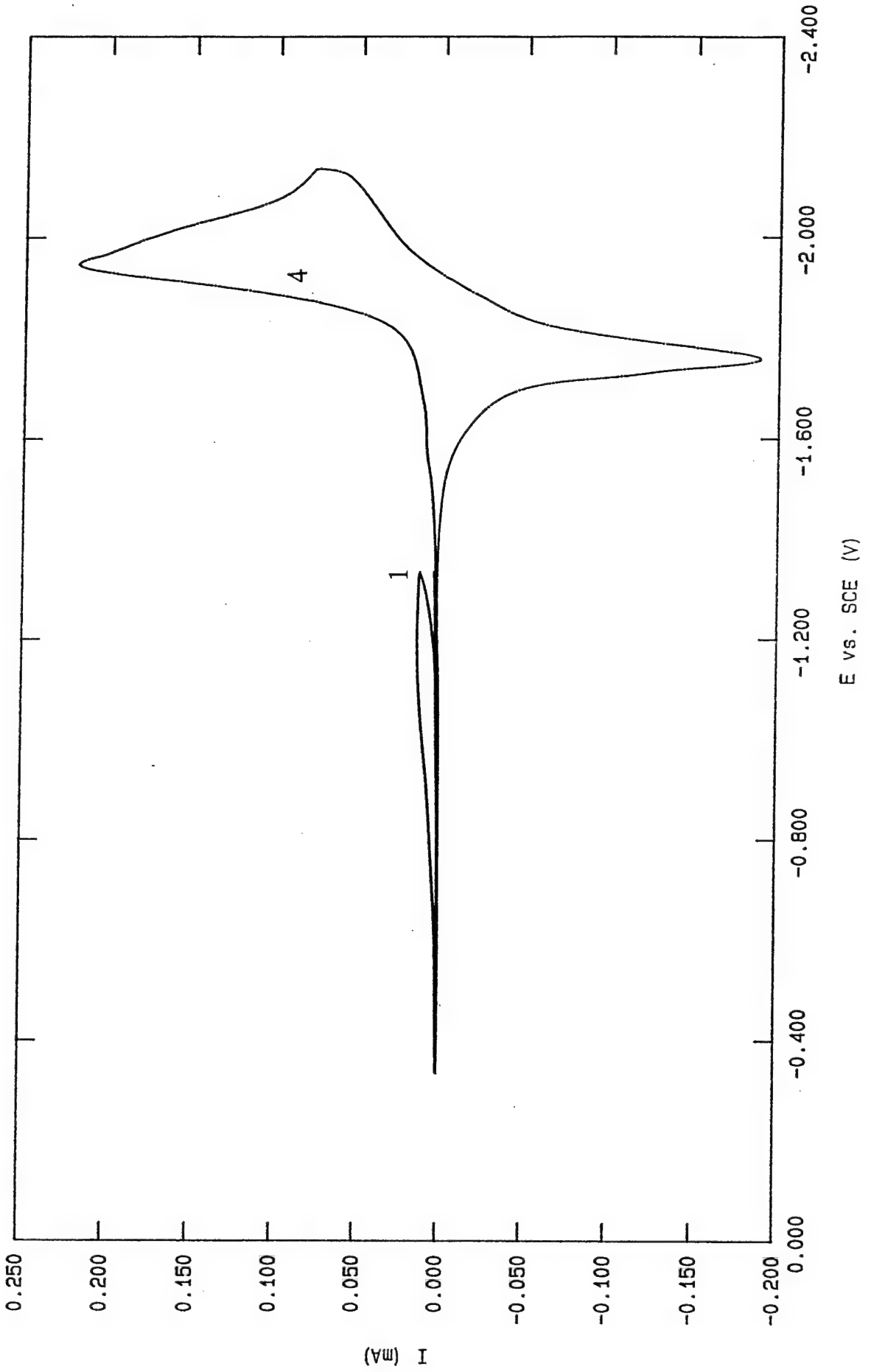
0.250
0.200
0.150
0.100
0.050
0.000
-0.050
-0.100
-0.150
-0.200
I (mA)
0.000
-0.400
-0.800
-1.200
-1.600
-2.000
-2.400
E vs. SCE (V)
4
1

Figure 2

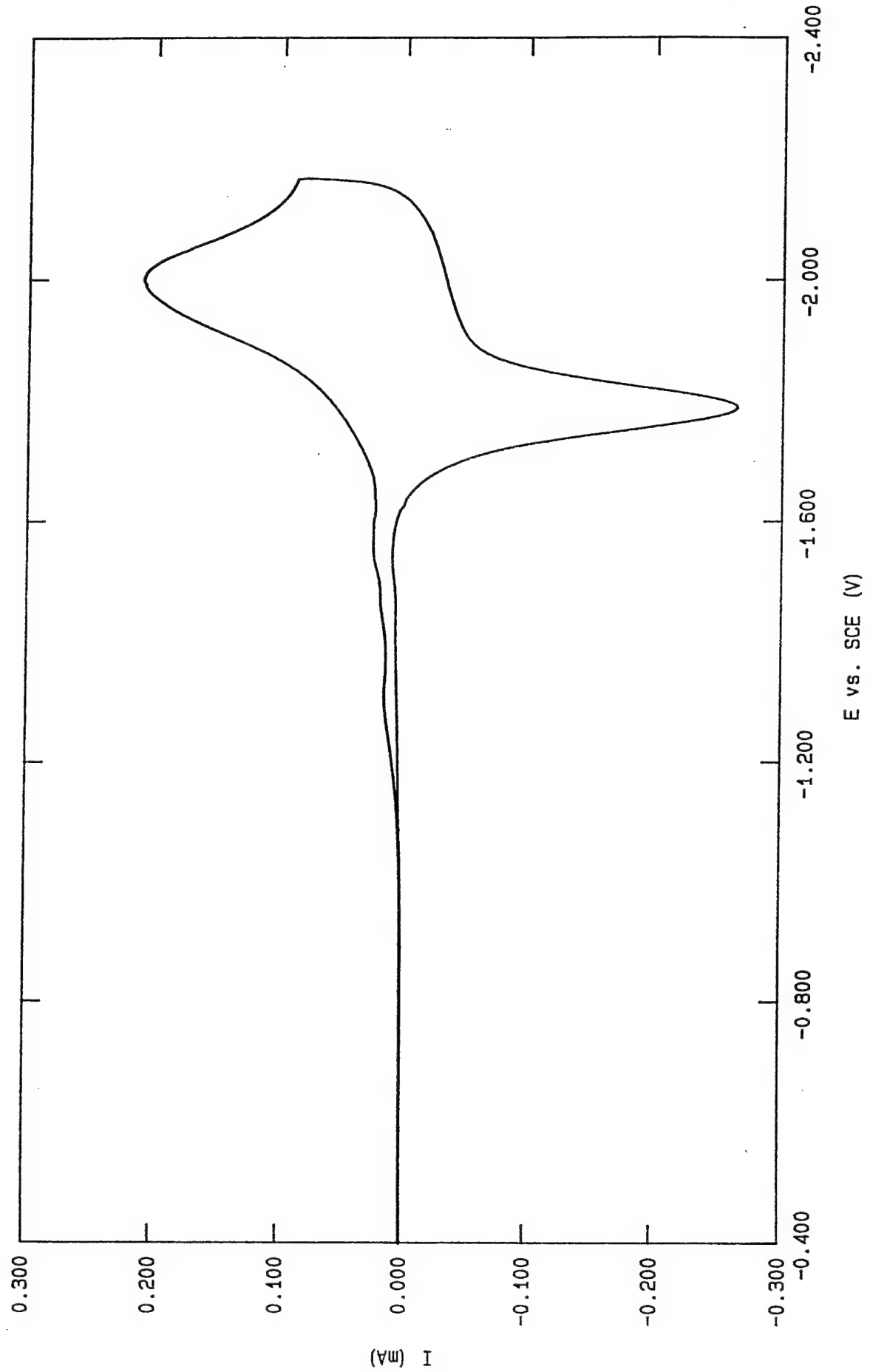
0.300
0.200
0.100
0.000
-0.100
-0.200
-0.300
I (mA)
-0.400
-0.800
-1.200
-1.600
-2.000
-2.400
E vs. SCE (V)

Figure 3

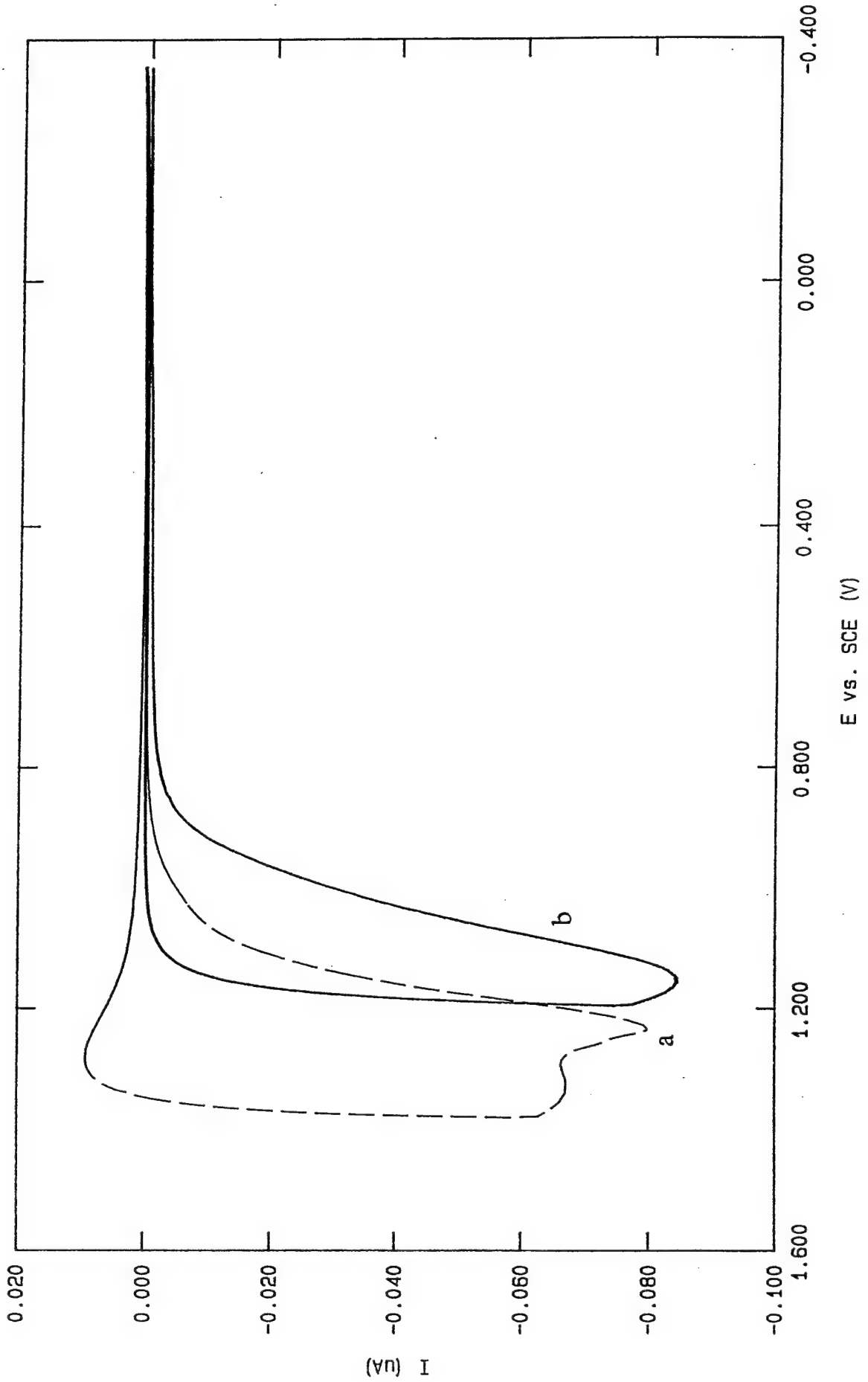
0.020
0.000
-0.020
-0.040
-0.060
-0.080
-0.100
I (uA)
-0.400
0.000
0.400
0.800
1.200
1.600
E vs. SCE (V)
a
b

Figure 4

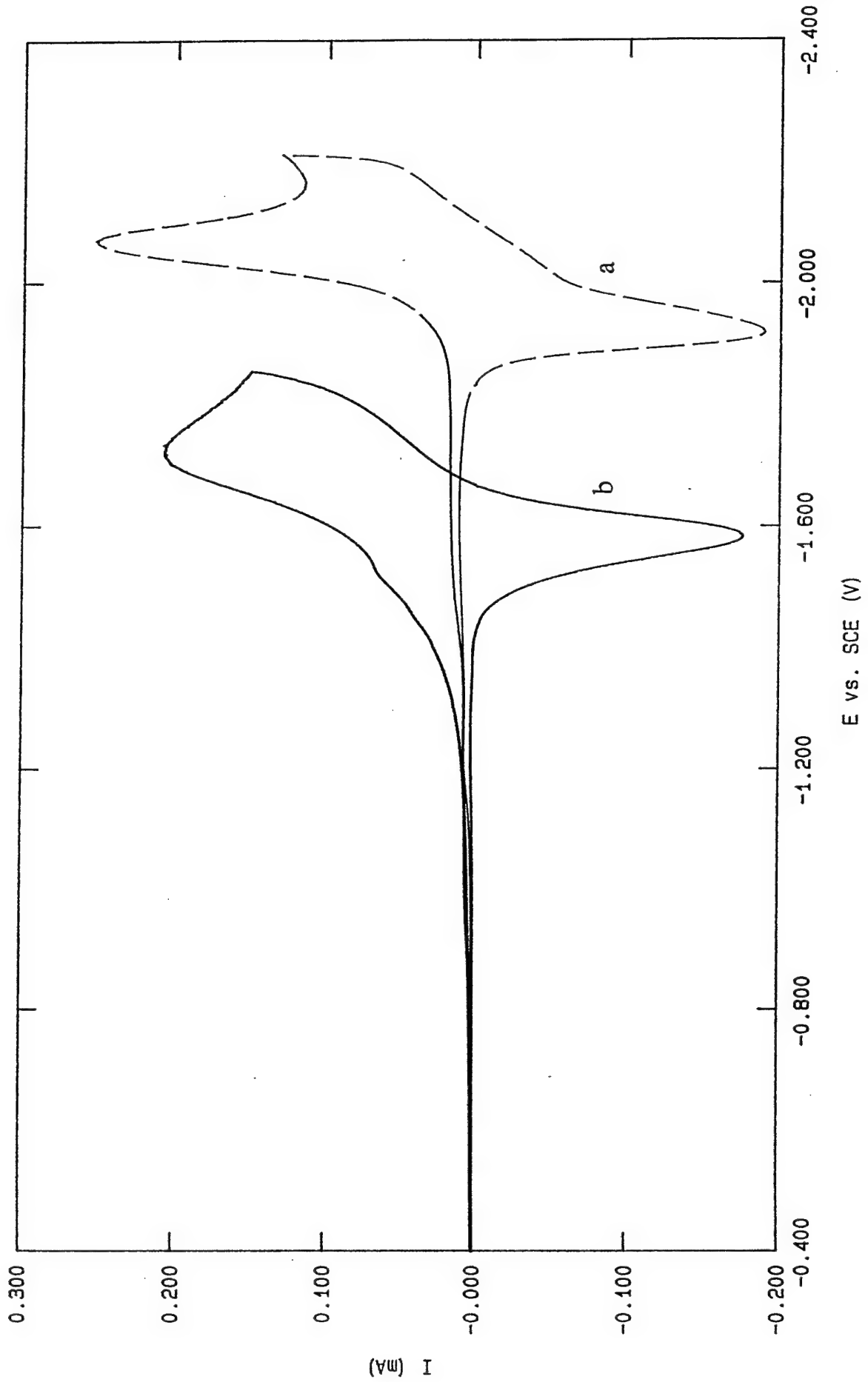
0.300
0.200
0.100
-0.000
-0.100
-0.200
I (mA)
-2.400
-2.000
-1.600
-1.200
-0.800
-0.400
E vs. SCE (V)
a
b

FIGURE 5

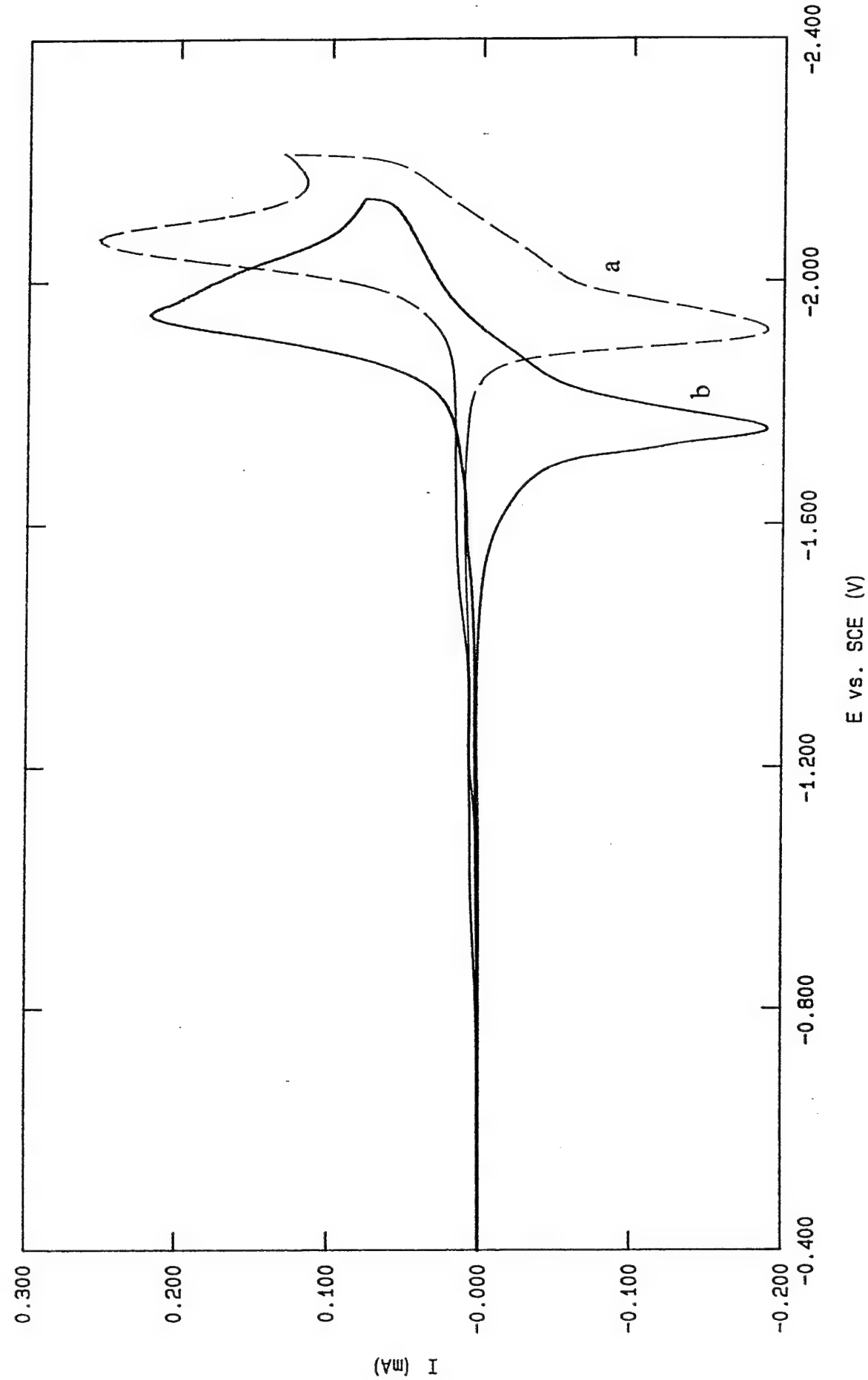
-2.400
-2.000
-1.600
-1.200
-0.800
-0.400
E vs. SCE (V)
a
b
0.300
0.200
0.100
-0.000
-0.100
-0.200
I (mA)

FIGURE 6

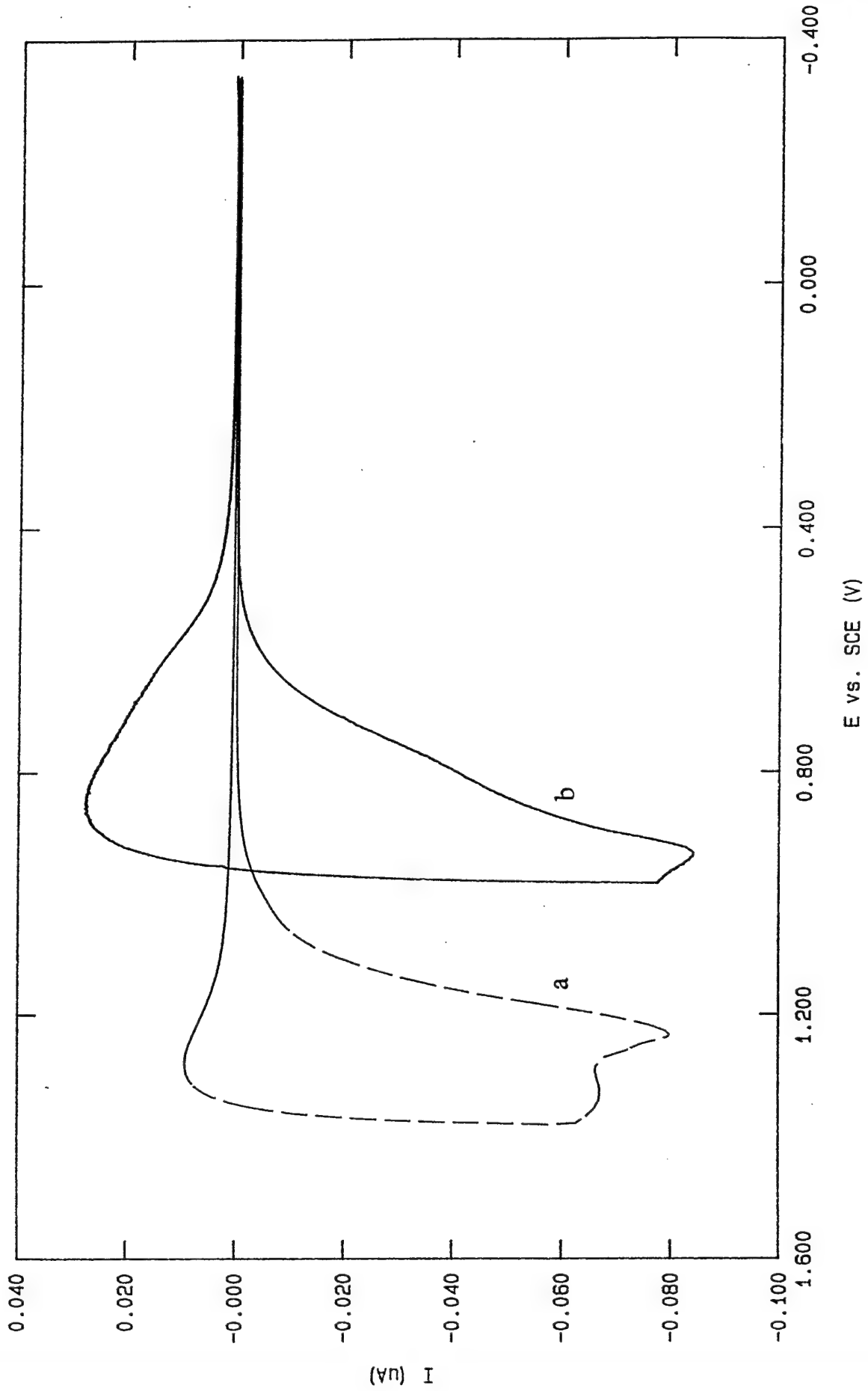
0.040
0.020
-0.000
-0.020
-0.040
-0.060
-0.080
-0.100
I (uA)
1.600
1.200
0.800
0.400
0.000
-0.400
E vs. SCE (V)
a
b

FIGURE 7

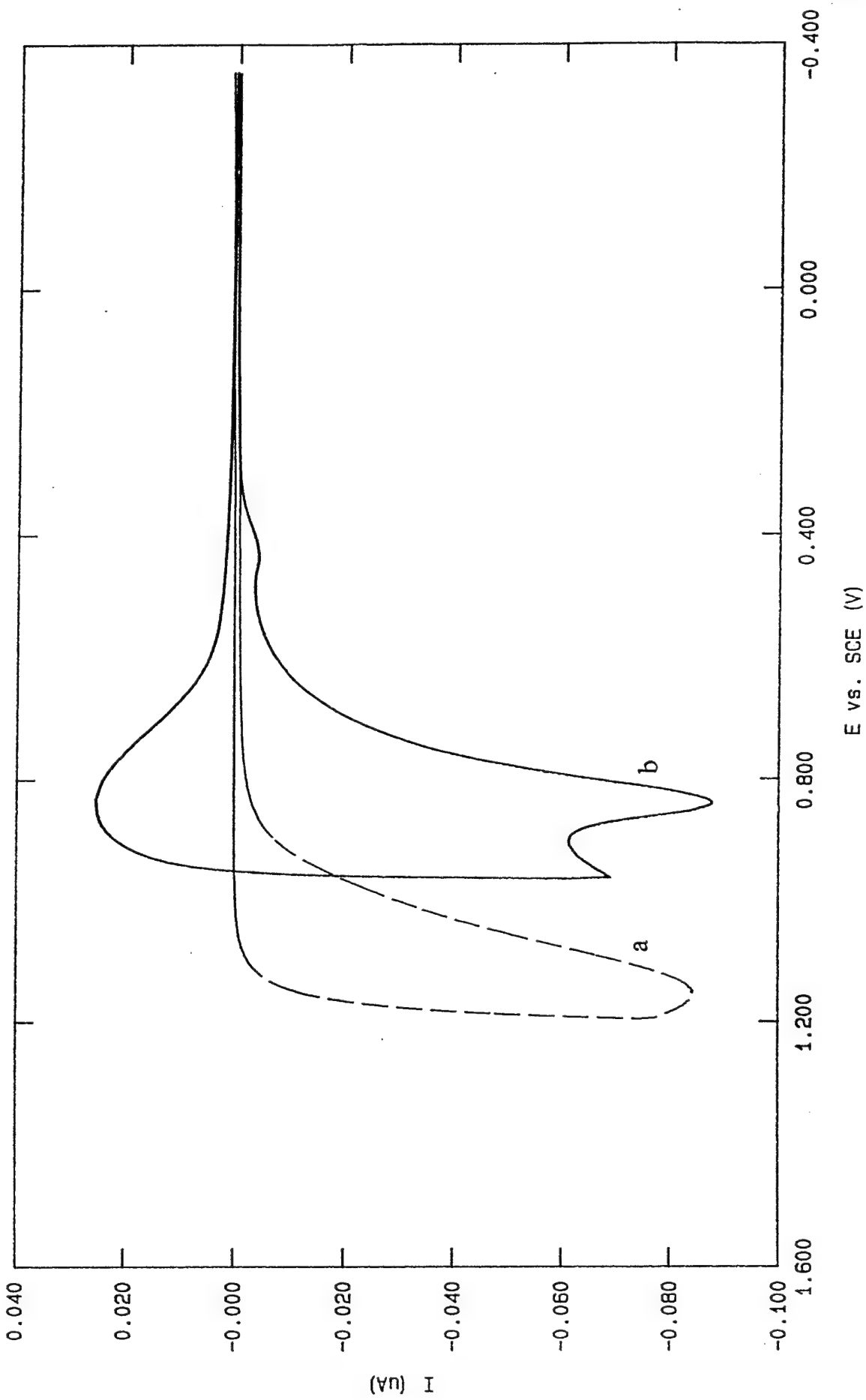
0.040
0.020
-0.000
-0.020
-0.040
-0.060
-0.080
-0.100
I (uA)
1.600
1.200
0.800
0.400
0.000
-0.400
E vs. SCE (V)
a
b

FIGURE 8

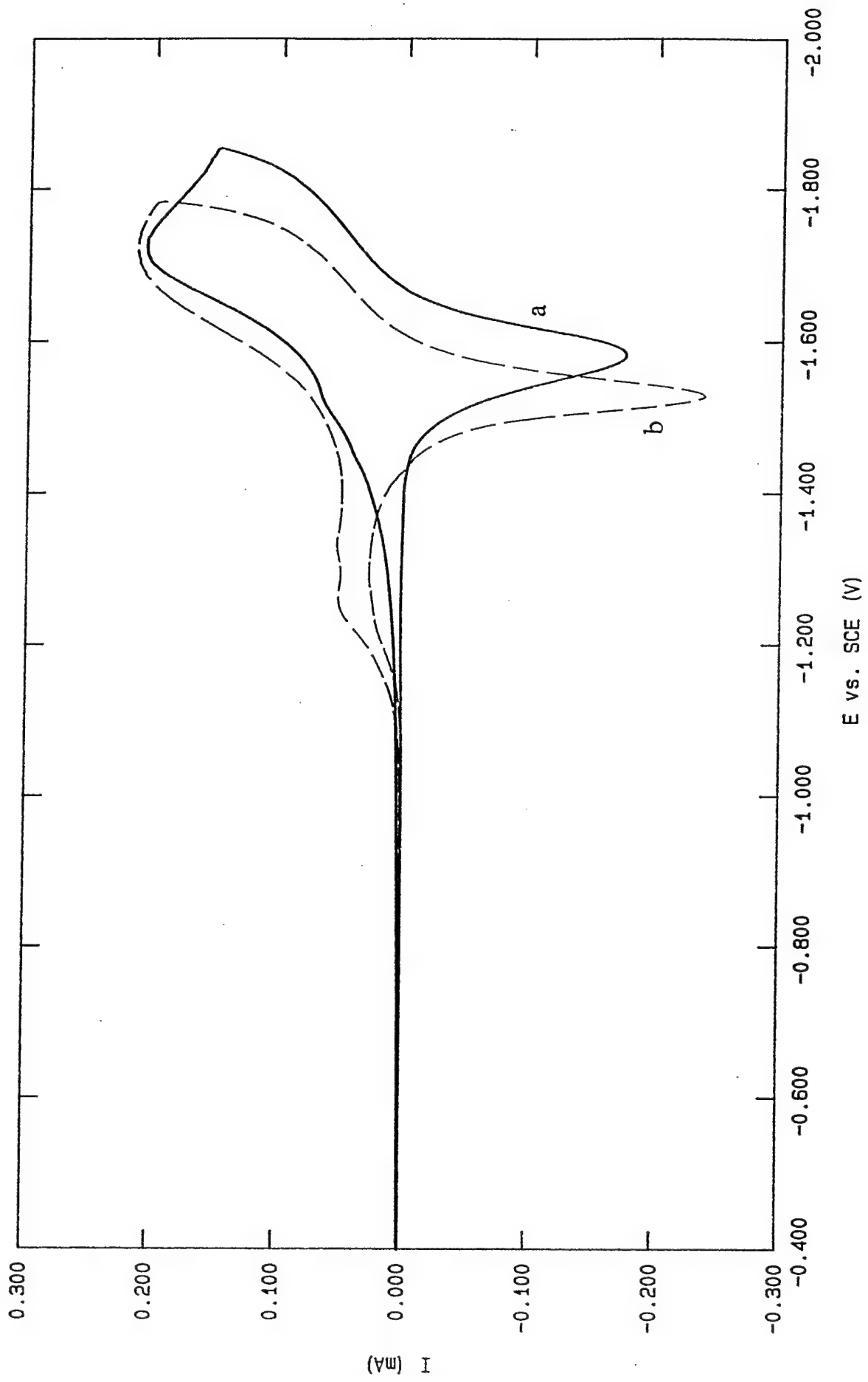
0.300
0.200
0.100
0.000
-0.100
-0.200
-0.300
I (mA)
-0.400
-0.600
-0.800
-1.000
-1.200
-1.400
-1.600
-1.800
-2.000
E vs. SCE (V)
a
b

FIGURE9

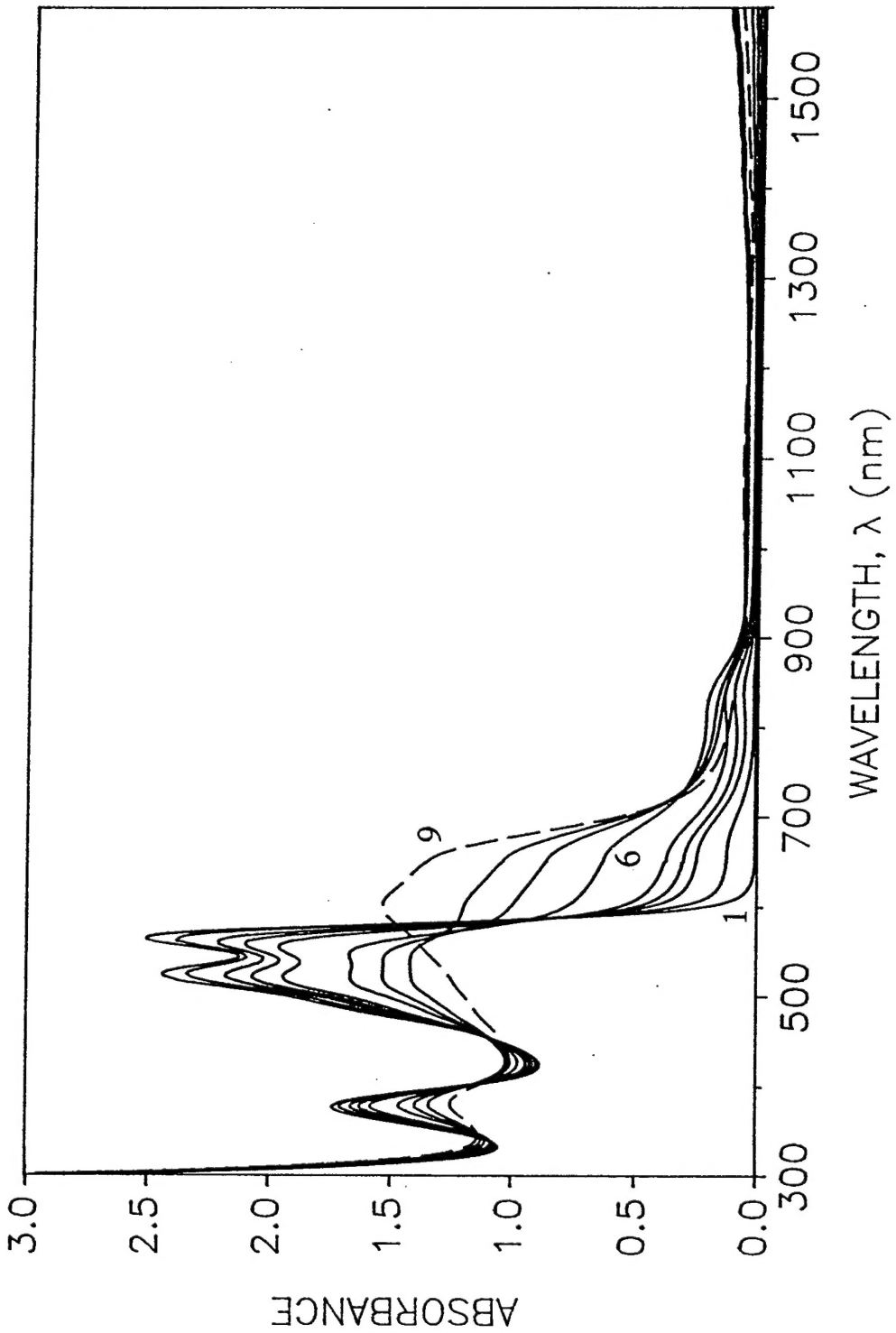
ABSORBANCE
3.0
2.5
2.0
1.5
1.0
0.5
0.0
300
500
700
900
1100
1300
1500
WAVELENGTH, λ (nm)
1
6
9

FIGURE 10

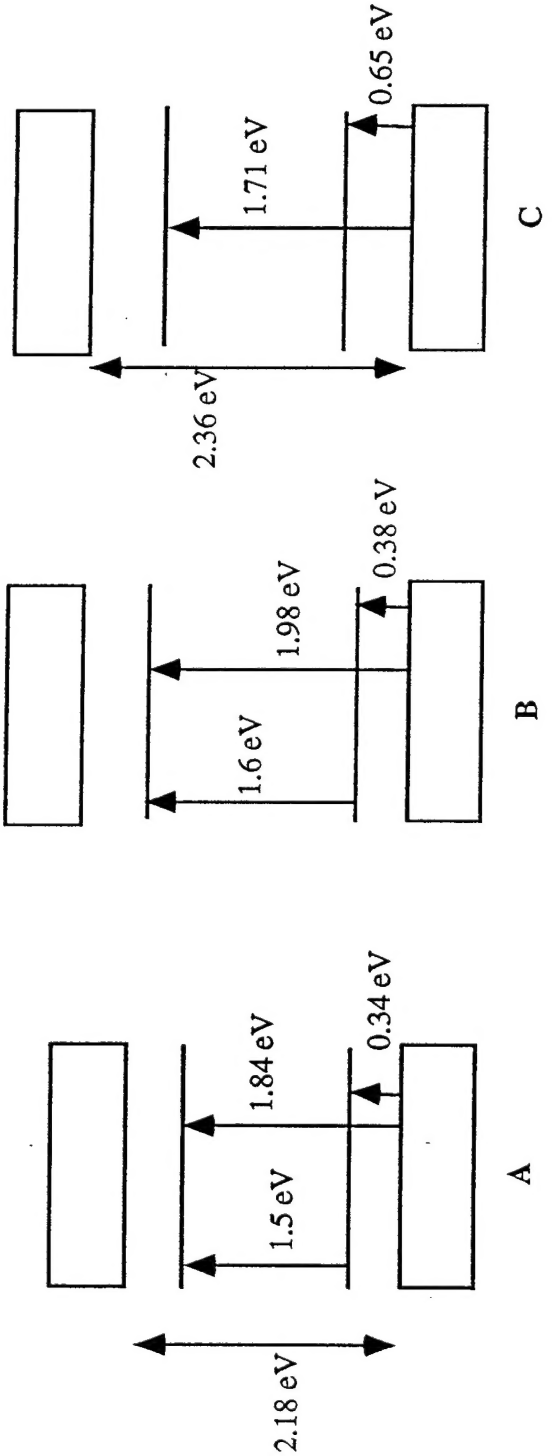
2.18 eV
1.5 eV
1.84 eV
0.34 eV
A
1.6 eV
1.98 eV
0.38 eV
B
2.36 eV
1.71 eV
0.65 eV
C

FIGURE 11

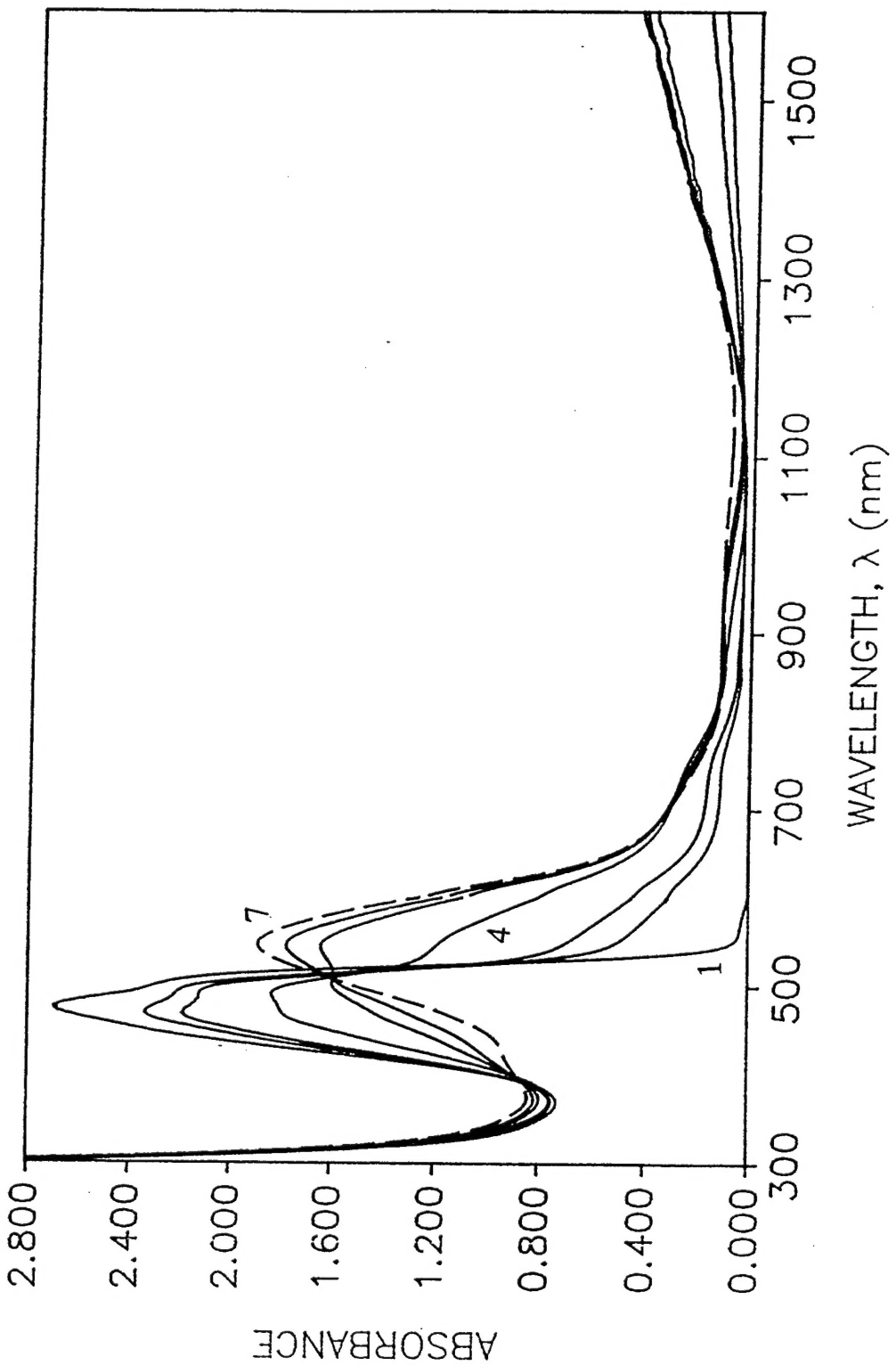
ABSORBANCE
2.800
2.400
2.000
1.600
1.200
0.800
0.400
0.000
300
500
700
900
1100
1300
1500
WAVELENGTH, λ (nm)
7
4
1

FIGURE 12

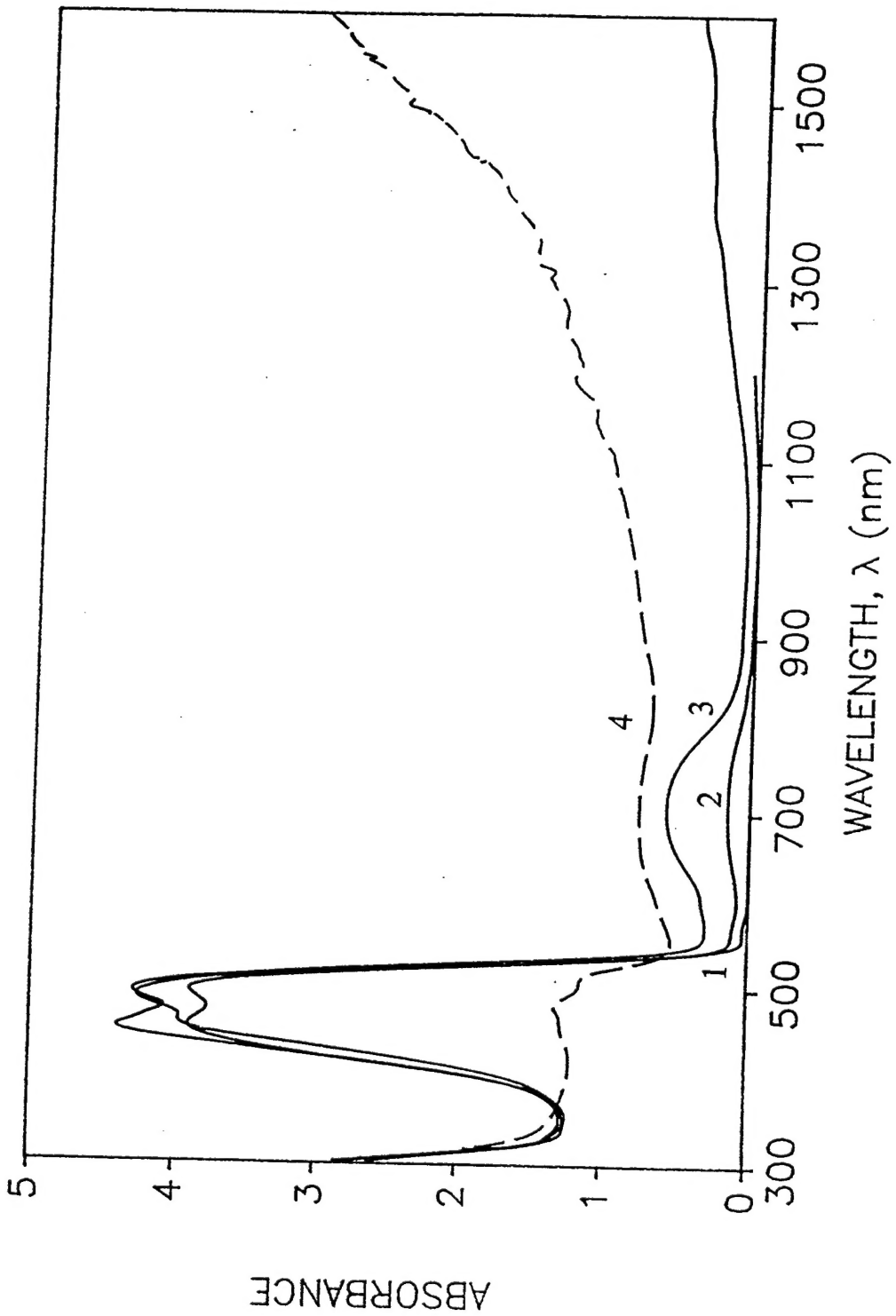
ABSORBANCE
0
1
2
3
4
5
300
500
700
900
1100
1300
1500
WAVELENGTH, λ (nm)
1
2
3
4